Chemical Science

Cite this: *Chem. Sci.*, 2012, **3**, 1162

www.rsc.org/chemicalscience

EDGE ARTICLE

How does a supramolecular polymeric nanowire form in solution?†

Ting Lei,[a] Zi-Hao Guo,[a] Cui Zheng,[b] Yue Cao,[a] Dehai Liang*[b] and Jian Pei*[a]

Received 28th December 2011, Accepted 15th February 2012
DOI: 10.1039/c2sc01123a

Supramolecular polymerization follows a nucleation-elongation mechanism; however, after the supramolecular polymerization, what happens while forming nanowires? In order to answer this question, we systematically investigated the molecular packing and growth mechanism of a series of supramolecular polymeric nanowires. We carefully analyzed the molecular packing in the nanowires and proposed a packing model through X-ray diffraction (XRD) and high-resolution transmission electron microscopy (HR-TEM). We used dynamic light scattering (DLS) to investigate *in situ* the growth process of these nanowires. The DLS results showed that after nucleation growth, a mesoscale assembly existed as an intermediate, which then formed the nanowires. This is the first example to directly monitor the growth of organic nanowires in solution. We also investigated the solvent effect on the self-assembly process of the side-chain functionalized monomers. Our investigation demonstrates that the weaker the interactions between the lateral groups, and the stronger the interactions of the lateral groups with the solvent are, the more obvious the tendency to 1D growth. Based on these results, we proposed that an "oriented-attachment" growth mechanism existed in this system after the supramolecular polymerization. Furthermore, single molecular nanowires and side-by-side attached single molecular nanowires were also observed through atomic force microscopy (AFM), which further supported the "oriented-attachment" mechanism. Accordingly, we demonstrate that after the supramolecular polymerization, "oriented attachment" growth mechanism is another critical process for the construction of large anisotropic organic assemblies, such as organic nanowires.

Introduction

Organic nanowires (ONWs) have attracted increasing attention due to their potential application as a new bottom-up approach to construct nano/micro optoelectronic devices,[1] such as explosive detection,[2] organic field-effect transistors,[3] and photowaveguide materials.[4] Compared to their inorganic counterparts, organic materials provide advantages including unlimited choices of building blocks, versatile modification of materials from molecular level, high flexibility, low cost, and ease for large-area fabrication.

Because the morphology and crystallinity of nanowires are important for their optoelectronic properties, understanding the growth mechanism is essential to control the growth of ONWs. Lehn and co-workers observed that tartaric acid derivatives formed some small nuclei followed by the growth of the nuclei into helical filaments *via* chiral self-assembly.[5] Moore and Zhao investigated the nucleation-elongation process in the polymerization of *m*-phenyleneethynylene (*m*PE). The process was driven by the folding energy when the foldamers grew *via* imine metathesis.[6,7] Meijer and co-workers studied the self-assembly of oligo(*p*-phenylenevinylene) derivatives by circular dichroism spectroscopy, and proposed that the nucleation-elongation polymerization was a thermo-activated equilibrium process instead of an isodesmic one, which was also strongly dependent on the solvent structure.[8] The growth of some other supramolecular polymeric systems were also demonstrated to follow similar nucleation-elongation processes.[9,10] Accordingly, nucleation-elongation polymerization is ubiquitous in supramolecular chemistry and various molecular interactions including hydrogen-bonding, π–π interaction, and even dynamic covalent bonding act as the main driving force. However, these investigations were mostly focused on the process of supramolecular polymerization, the formation mechanism of further larger aggregates, such as ONWs, was seldom investigated.

The growth of ONWs, especially those with hundred nanometre size, is usually considered as a confined crystallization process. Many interactions, such as π–π stacking,[11] donor–acceptor[12] and hydrophobic interactions,[13] were utilized to control the anisotropic growth of organic nanomaterials.

[a]*Beijing National Laboratory for Molecular Sciences (BNLMS), the Key Laboratory of Bioorganic and Molecular Engineering of the Ministry of Education, College of Chemistry and Molecular Engineering, Peking University, Beijing 100871, China. E-mail: jianpei@pku.edu.cn; Fax: (+86)-10-62758145; Tel: (+86)-10-62758145*
[b]*The Key Laboratory of Polymer Chemistry and Physics of the Ministry of Education, College of Chemistry and Molecular Engineering, Peking University, Beijing 100871, China*

† Electronic supplementary information (ESI) available: experimental details, concentration-dependent UV-*vis* and PL spectra, SEM images, and molecular modelling. See DOI: 10.1039/c2sc01123a

Classically, the growth of crystals was thought to occur through molecule-by-molecule addition to the surface of nuclei. Meanwhile, unstable phases (small particles and metastable polymorphs) are dissolved, and then reprecipitate into more stable phases.[14] This process, called "Ostwald ripening", are widely accepted to describe the crystallization process of inorganic or organic crystals (Fig. 1, Pathway A).[15] In contrast to the traditional "Ostwald ripening" mechanism, Penn and Banfield proposed an "oriented-attachment" growth mechanism for inorganic nanostructures, in which bigger particles grew from small primary nanoparticles through a highly oriented fashion.[16–18] In this process, nuclei first form some primary assemblies. For inorganic primary assemblies, they can be further stabilized by organic molecules, and then form mesocrystals through "oriented-attachment". Since the mesocrystals are already crystallographically aligned, the fusion of the particles to form single crystals is thermodynamically favored (as shown in Fig. 1, Pathway B and C). The "oriented-attachment" mechanism has been widely applied to the anisotropic growth of inorganic nanocrystals, such as inorganic nanorods,[19] inorganic hollow materials,[20] and metal organic frameworks.[21] However, this mechanism has rarely been tested in organic supramolecular systems, especially in the growth of organic nanomaterials.

We developed a three-dimensional (3D) structure, which has a shape-persistent structure with three conjugated arms perpendicular to a planar core.[22] The direction of three arms was designed as the self-assembly direction, and the planar core can be modified with different functional groups. After incorporating carboxylic groups, we obtained molecule **1-C12** (as shown in Scheme 1, blue one). It formed supramolecular polymeric nanowires through multiple hydrogen-bonding and exhibited high solid-state fluorescent quantum efficiency.[23a] Although the supramolecular polymeric nanowires of **1-C12** were obtained, detailed analysis of the structure and the growth mechanism of the nanowires is still obscure. We also developed a synthetic method to functionalize the nanowires and obtained four novel monomers, **1-TPP**, **1-BTTPA**, **1-BTHex**, and **1-BTMe** to investigate the self-assembly processes.[23b]

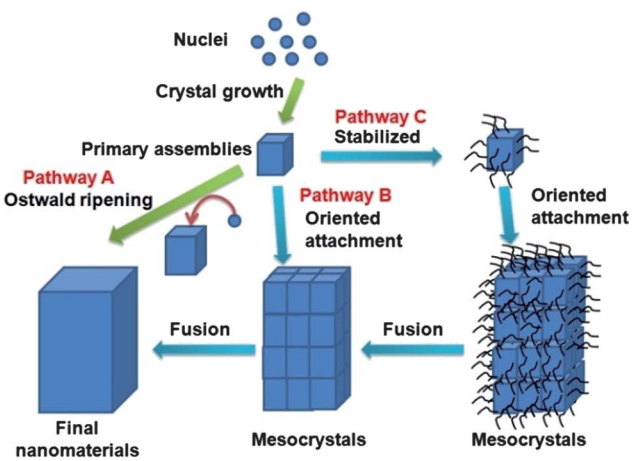

Fig. 1 Schematic representation of the classical and the oriented-attachment crystallization. Pathway A: classical Ostwald ripening pathway; Pathway B: oriented attachment of primary particles; Pathway C: primary particles stabilized with organics.[17,18]

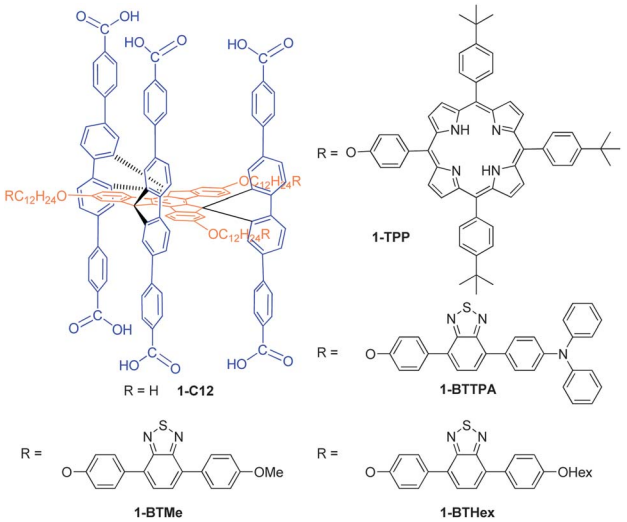

Scheme 1 Molecular structures of the monomers used in this study.

Herein, we propose that the growth of organic nanowires follows the nucleation-elongation polymerization and then the oriented-attachment growth mechanism. In the first part, we analyze the molecular packing of the nanowires by using X-ray diffraction (XRD) and high-resolution TEM (HR-TEM) and propose a molecular packing model. Then dynamic light scattering (DLS) is employed to investigate *in situ* the growth process of the nanowires. The DLS results show that the growth of the nanowires obeys a nucleation-elongation process and a mesoscale assembly exists as an intermediate, which then forms the nanowires. A trimodal distribution in DLS characterization suggests that the supramolecular polymerization and the nanowire growth are both not isodesmic processes. Moreover, we discover a solvent effect on the self-assembly process of the lateral functionalized monomers. All the results support our proposed mechanism that an oriented-attachment mechanism exists in the growth of organic nanowires, after the supramolecular polymerization. Noticeably, this is the first example to employ the "oriented-attachment" mechanism to explain the growth of organic nanomaterials.

Results and discussion

Molecular packing in nanowires formed by 1-C12

The nanowires of **1-C12** were obtained either by slowly cooling down its THF solution, or by slowly diffusing hexane vapour into the THF solution. Fig. 2a shows the SEM image of the nanowires of **1-C12**. The nanowires were uniform with high aspect ratio, about hundreds of nanometres in width and several micrometres in length. If we added a small portion of a proton-accepting or donating solvent, such as H_2O, methanol or DMSO, the nanowires broke into short cylinders. This result indicates that the hydrogen-bonding direction is along the long-axis of the nanowires. After carefully controlling the growth condition of the nanowires, better crystallized nanowires were obtained. The HR-TEM image of nanowires formed by **1-C12** showed that there was well-ordered packing along the nanowires, especially in the middle of the nanowires (Fig. 2b). Fast Fourier

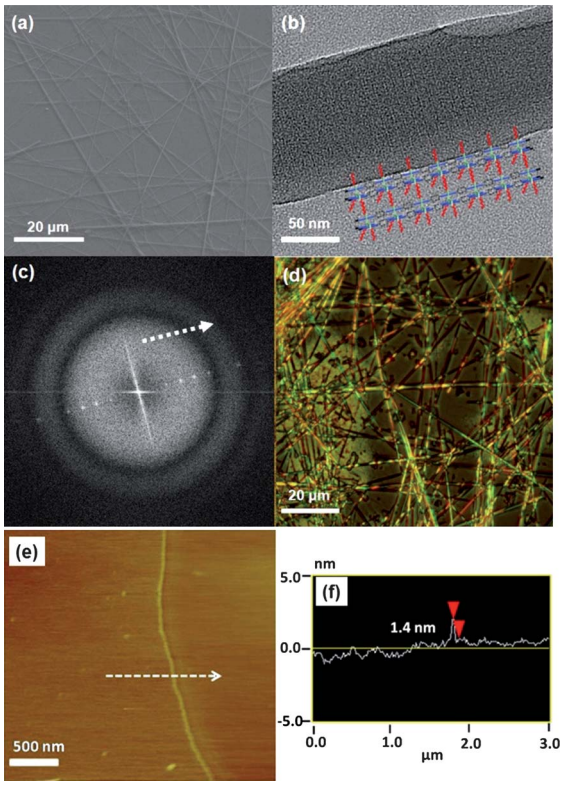

Fig. 2 (a) SEM and (b) TEM images of the nanowires formed by **1-C12**; (c) FFT image of the TEM image; (d) POM image of nanowires. The nanowires were formed by diffusing hexane into the THF solution of **1-C12** (1 mg mL^{-1}); (e, f) AFM height images of an air-dried sample of a highly diluted solution of **1-C12** (10^{-6} M) in THF/Cl2CHCH$_2$Cl$_2$ (1 : 1) deposited on a mica substrate.

transformation (FFT) was employed to analyze these nanowires (Fig. 2c). We used the reciprocal space generated by FFT to understand the molecular packing. A series of diffraction points was observed in the FFT image indicating that there is some periodicity along the nanowires. Polarized optical microscopy (POM) showed that the nanowires had obvious birefringence, which indicated anisotropic molecular packing in the nanowires.

After diluting the concentration of **1-C12** solution to 10^{-6} mol L^{-1}, interestingly we observed single molecular wires using AFM after drop-casting highly diluted solution onto a mica substrate (Fig. 2e). This result suggests that **1-C12** has a shape-persistent structure and strong interactions merely exist in one direction. To obtain detailed molecular packing information in the nanowires, we used out-of-plane XRD to analyse these nanowires. Although the powders of **1-C12** directly precipitated from THF solution showed many diffraction peaks (Fig. 3a), the nanowires of **1-C12** astonishingly exhibited no obvious diffraction peak (Fig. 3b). Only two broad peaks at 4.5° and 22° were observed, signifying a *d*-spacing of 19.6 and 4.0 Å, respectively. 19.6 Å is consistent with the molecular size of **1-C12**, while 4.0 Å is a typical van der Waals interaction distance. Based on the above results, we proposed that the nanowires were formed by a bundle of single molecular wires through lateral van der Waals interactions, and the single molecular wires were formed by hydrogen-bonding of **1-C12** molecules. However, why are the diffractions of the nanowires much weaker than that of the powders? To answer this question, we illustrated a cartoon to explain the relationship between molecular packing and diffraction. As shown in Fig. 3c, because the nanowires were formed by a bundle of single molecular wires and the lateral van der Waals interaction was weak and non-directional, periodicity only existed along the hydrogen-bonding direction. Consequently, XRD did not detect any observable periodicity but TEM can. Such kind of packing in nanowires is similar to the nematic phase in liquid crystal. For a typical nematic phase, molecules tend to be parallel to some common axis and, because the centers of the molecules have no long-range orders there is only diffuse scattering in XRD.[24] In the nanowires, all the single molecular wires tend to be parallel with each other to maximize van der Waals interactions and minimize the intermolecular vacuum. In other words, single molecular wires formed a nematic phase in the nanowire. The single molecular wires are not well crystallized, which maybe result from the weak and non-directional lateral interactions and some kinetic problems. The kinetic problems may originate from the large molecular size of **1-C12** or the formation mechanism of the nanowires discussed later.

Monitoring the growing process of 1-C12 nanowires by DLS

To understand the growth mechanism of the nanowires, we first performed concentration-dependent and time-dependent UV-*vis* and NMR spectra to investigate the self-assembly process of **1-C12**. However, unlike other π–π stacking systems, UV-*vis* and NMR spectra of **1-C12** showed no obvious change in the experiment (Fig. S1†), possibly because the nanowires were formed by hydrogen-bonding and the molecule has a shape-persistent structure. Thus we employed DLS to *in situ* monitor the self-assembly of the monomers. **1-C12** stayed as individual molecule in THF at 1.0×10^{-4} mol L^{-1} after being refluxed for more than 10 min. The hydrodynamic radius was about 1 nm, and no prominent aggregate was observed at 25 °C right after reflux (Fig. 4b). However, **1-C12** assembled in THF with time under such conditions. Fig. 4a shows the time dependence of the excess scattered intensity of **1-C12**. An "S" curve followed by a heavy fluctuation after 60 min was observed. The "S" curve suggested the occurrence of nucleation and growth.[25,26] In the first 12 min, the excess scattered intensity kept constant at about 40k counts per second. Beside single monomers, certain aggregates were also observed in this stage (Fig. 4c). Since the scattered intensity is roughly proportional to the sixth power of particle size, the aggregate formed in this stage was extremely small. After 12 min, a sharp increase in the excess scattered intensity occurred, indicating the fast growth of particles in solution. After about 1 h, a heavy fluctuation of scattered intensity was observed. At this stage, two kinds of aggregates with sizes of 100 nm and 10 μm were formed, coexisting with the monomers. The heavy intensity fluctuation was mainly caused by the Brownian motion of the 10 μm aggregates.

To clarify the two aggregates ($R_{h,app}$ of 100 nm and 10 μm), we investigated the growth of the monomers in dilute solution (1×10^{-6} mol L^{-1}). After the same growing process, we only observed two peaks in the solution, and very large aggregates (>10^4 nm) did not appear in dilute solution (Fig. 4e). Additionally the 100 nm size assemblies were relatively less. This size distribution indicates that the formation of the 100 nm aggregates was

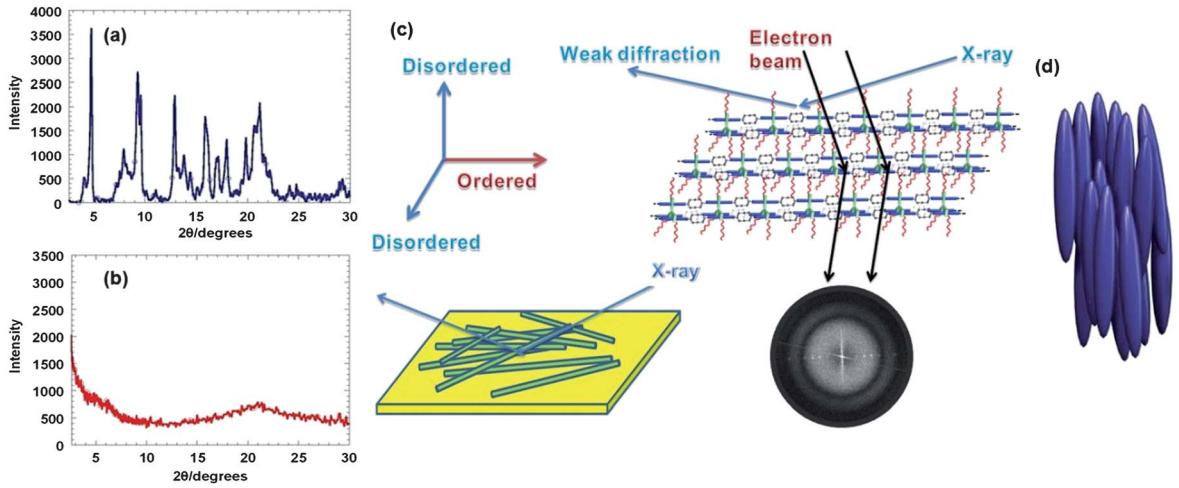

Fig. 3 Out-of-plain XRD spectra of (a) powders (directly precipitated from solution) and (b) nanowires of **1-C12**; (c) cartoon representation of the molecular arrangement in the nanowires, and diffraction mechanism of XRD and SAED; (d) cartoon representation of a typical nematic phase.

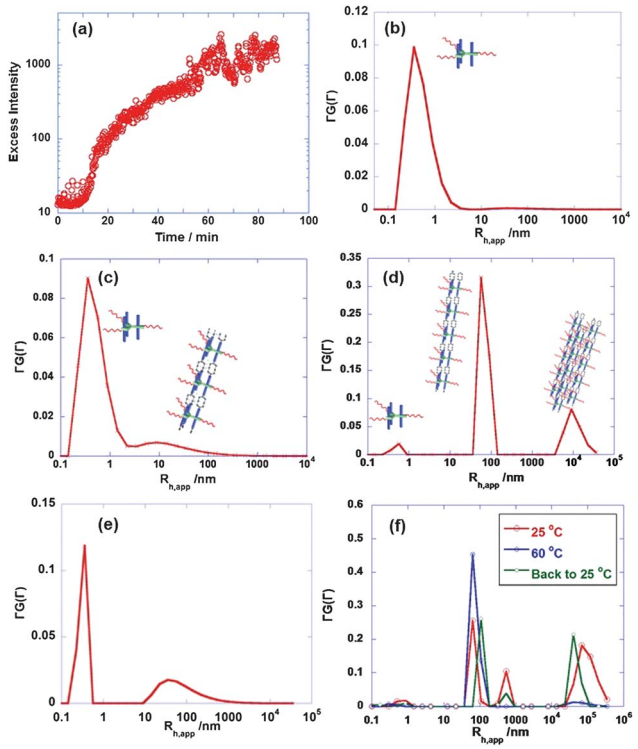

Fig. 4 (a) Time dependence of the excess scattering intensity of **1-C12** in THF at 1.0×10^{-4} mol L^{-1}; the size distribution of (b) the fully dissociated single molecule; (c) after 5 min growth and (d) after 80 min growth. The cartoons are the proposed molecular aggregates assigned to different peaks. (e) Size distribution of **1-C12** in THF (a) at dilute solution (1×10^{-6} mol L^{-1}) and (f) at different temperature in high concentration (1×10^{-4} mol L^{-1}).

distinctly different from isodesmic behaviour, because no short oligomers (in the range of 1–10 nm) were observed in the solution.

It is reasonable to ask the question whether the size distributions in Fig. 4d are true equilibrium states. Thus we also studied the temperature effect on the aggregates by heating and cooling the solution between fixed temperatures at high concentration (1×10^{-4} mol L^{-1}). **1-C12** in THF was firstly kept at 25 °C for several hours to ensure the growth of the aggregates. As shown in Fig. 4f, a trimodal distribution was observed in the system. The solution was then heated at 60 °C for 30 min, the aggregates with size more than 10 μm were almost disappeared, while the 100 nm aggregates remained and became the dominant component in the system. At last, we cooled the solution at 25 °C for 30 min, and the aggregates with sizes more than 10 μm came out again, and the area ratio of the 100 nm aggregates was correspondingly decreased. Noticeably, the aggregates around 500 nm sometimes appeared in the experiment, which was attributed to some larger aggregates, but they were not thermodynamically stable. This temperature cycle suggests that the size distribution was thermodynamically stable in the solution and the growth process of nanowires were not an isodesmic step-growth process, which is similar to previous findings by Moore *et al.*[6]

The curves in Fig. 4e and 4f suggest that the 100 nm aggregates formed by **1-C12** in THF have a tendency to further aggregate at both higher concentration and lower temperature, and the driving forces for the two aggregates are different in nature. As discussed above, single molecular wires with hundreds of nanometres in length were observed in dilute solution and nanowires were formed by a bundle of single molecular wires at elevated concentration. With further consideration that the major intermolecular attraction forces of **1-C12** are hydrogen-bonding and van der Waals interactions, we attributed the primary aggregates (100 nm) to rigid rod single molecular nanowires and the secondary aggregates (10 μm) to the broader nanowires, as indicated by the cartoon in Fig. 4. Therefore, the trimodal distribution indicated that the formation processes of supramolecular polymers (100 nm) and the nanowires (10 μm) were both not isodesmic. Previously, isodesmic growing mechanism was only observed in the polymerization process,[8] but herein we found that after the polymerization the formation of nanowires was also isodesmic.

We also understood this process from the perspective of Gibbs free energy change. The classical model of crystallization considers crystal growth as an amplification process in which

stable nuclei are enlarged by replicating unit cell. The Gibbs energy barrier is the activation energy of nucleation (Fig. 5a). Nuclei larger than the critical size (r^*) further decrease their free energy to form crystals, while nuclei smaller than the critical size dissolve because of high surface area.[17] However, in our system, we observed the "S" curve in DLS, indicating a nucleation-growth happened. r_1^* in Fig. 5b shows this activation barrier, which is similar to the reported supramolecular polymerization process reported in other systems.[6–10] Because the multiple hydrogen-bonding is much stronger than the van der Waals interaction, this polymerization process is kinetically and thermodynamically favourable. Thus, the excess scattering light increased quickly at this process, and a kind of mesoscale primary assembly (100 nm size) was formed in solution. Compared to the van der Waals force among single molecular wires, the entropy effect is dominated in dilute solution and higher temperature, so we only observed the 100 nm aggregates. As concentration increases or temperature decreases, the barrier r_2^* was overcome and single molecular wires tend to aggregate, leading to the final nanowires. Accordingly, the results from DLS indicate that the self-assembly of **1-C12** in THF underwent a three-step process: (1) forming nuclei from small molecules; (2) forming primary single molecular nanowires *via* the elongation of the nuclei; (3) forming nanowires through further aggregation, just like the "oriented-attachment" mechanism in inorganic systems (Fig. 5b). As discussed above, this attachment process may cause kinetic problems and lead to the poor crystallinity of the nanowires because of the large size of the mesoscale primary assemblies.

Solvent effect on the self-assembly of nanowires

Inspired by the growth mechanism, we envisioned that the monomers preferred to form one-dimensional (1D) nanowires after introducing differently functional groups at the R_2 position. Therefore, we designed and synthesized four **1-C12** derivatives containing different fluorescent side-chain groups (Scheme 1). Herein, we systematically compare their different self-assembly process to understand solvent effects on 1D self-assembly and to reveal the "fusion" process after their "oriented attachment".

Vapor diffusion strategy was employed to grow the nanowires. This strategy needs a poor solvent with relatively low boiling point to diffuse into a good solvent with higher boiling point. All the monomers in Scheme 1 have moderate solubility in THF and are almost insoluble in hexane, dichloromethane (DCM) and chloroform. The four monomers were firstly dissolved in THF, and the poor solvent was then introduced by gas diffusion to gradually decrease the solubility. We first choose hexane as poor solvent to induce the growth of nanowires. However, the results were unexpected (Fig. S2†, a, c, e and g). Only **1-BTTPA** formed long nanowires, while other monomers formed aggregates with other morphologies. The aggregates of **1-TPP** and **1-BTMe** still kept some 1D growth tendency (Fig. S2†, a and e). Considering the oriented-attachment process, we envisioned that this unexpected result might be caused by the strong interaction between the lateral functional groups, which deteriorated the anisotropic 1D growth. Therefore, we changed the poor solvent to CH_2Cl_2 which is a good solvent for the side groups. Excitingly, both **1-TPP** and **1-BTMe** formed nanowires under this condition (Fig. S2†, b and f). **1-BTHex** also exhibited a strong 1D growth tendency (Fig. S2†, h).

To further understand this solvent effect, we propose that the lateral aggregation of the nanowires is determined by the intermolecular interactions of the side chains (Fig. 6a). One can imagine that once the lateral interaction becomes stronger, the lateral growth tendency will be reinforced. Fig. 6b displays the molecular models of the different side groups. **BTTPA** has a conical triphenylamine substructure, which hinders the π–π stacking of the side chains. **TPP** group has three 4-(*t*-butyl)-phenyl groups and shows less steric hindrance than the **BTTPA** one. **BTMe** group has a strong π–π interaction, thus we can hardly observe any nanowires when using hexane. The intermolecular interactions of **BTHex** became much stronger by incorporating hexyl groups. To comprehend the phenomena, we synthesized a model compound **DHBT**, which itself can assemble into nanowires because of π–π stacking and alkyl chain packing (Fig. 6c). Thus we did not observe satisfactory nanowires even

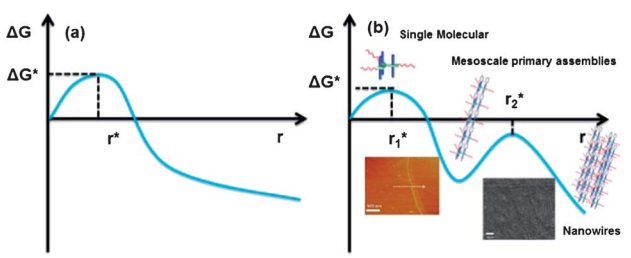

Fig. 5 Schematic representation of Gibbs free energy change of (a) classical nucleation-growth mechanism; (b) proposed three-step growth mechanism of **1-C12** nanowires. Inset picture is an AFM height image of a single molecular nanowire and the SEM image of **1-C12** nanowires.

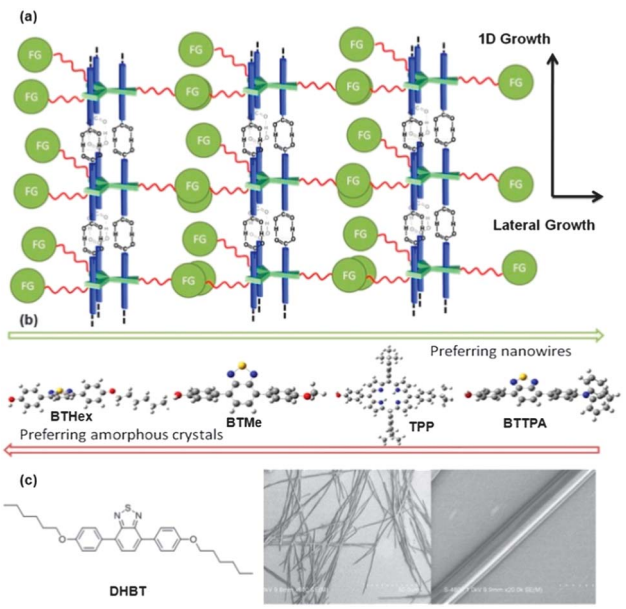

Fig. 6 (a) Cartoon representation of the lateral growth; (b) models of different side groups (molecular models are minimized using MMFF 94 force field); (c) molecular structure of dihexyl substituted benzothiadiazole derivatives (**DHBT**) and its SEM images of the **DHBT** nanowires grown by phase transfer methanol into the DCM solution of **DHBT**.

using CH_2Cl_2 as solvent. Based on these results, we conclude that the weaker the interactions between the lateral groups and the stronger the interactions of the side groups with the solvent are, the more obvious the tendency of the 1D growth shows. Therefore, the lateral interaction played a very important role in the lateral growth. Similar phenomena were also discussed in other supramolecular self-assembly systems.[27,28]

Single molecular wire packing and fusion process

TEM and AFM were employed to investigate the detailed information of the functionalized nanowires. As shown in Fig. 7a and 7d, nanowires of **1-TPP** and **1-BTTPA** were both formed by a bundle of single molecular nanowires. It was observed that these nanowires had many separated branches, greatly different from the nanowires of **1-C12** (Fig. 2b). SAED and FFT analyses did not give any observable periodicity for both kinds of nanowires, which indicated the nanowires were more amorphous than that of **1-C12**. However, nanowires of **1-C12** formed in dilute solution (10^{-5} M) were also observed with similar branches (Fig. 7g). Analogous results were also found in AFM images (Fig. 7b, and 7e). At a larger scale, **1-TPP** and **1-BTTPA** formed wires ranging from tens of nanometres to hundreds of nanometres in width. A detailed analysis by AFM revealed that the nanowires of **1-TPP** had the smallest height of 3.5 nm and those of **1-BTTPA** showed the smallest height of 3.8 nm (white arrows in Fig. 7). The heights agreed well with the size of the monomers given by molecular modelling (Fig. S3†), indicating the existence of single molecular wires. Previously we discussed that single molecular wires of **1-C12** were only observed in dilute solution (10^{-6} M), but herein the single molecular wires were found in concentrated solutions (10^{-4} M). Moreover, we also observed the lateral attached single molecular wires (red arrows) and fused nanowires (blue arrow). For instance, three parallel attached single molecular wires formed by **1-BTTPA** were observed in Fig. 7f. For **1-C12**, branched nanowires and single molecular wires were also observed in dilute solution (Fig. 7h and 7i), which was consistent with the DLS experiments in dilute solution. These results strongly support our proposed "oriented-attachment" mechanism. However, why did not **1-C12** form such kinds of branched structures but uniform nanowires in high concentration? We considered that the dodecyl chains are more flexible than those bulky and rigid functional groups, which made the fusion of single molecular wires of **1-C12** proceed more quickly. In contrast, the functionalized monomers **1-TPP** and **1-BTTPA** could not adjust their bulky functional groups to form tightly intermolecular packing, and thereby we observed their partially fused assemblies.

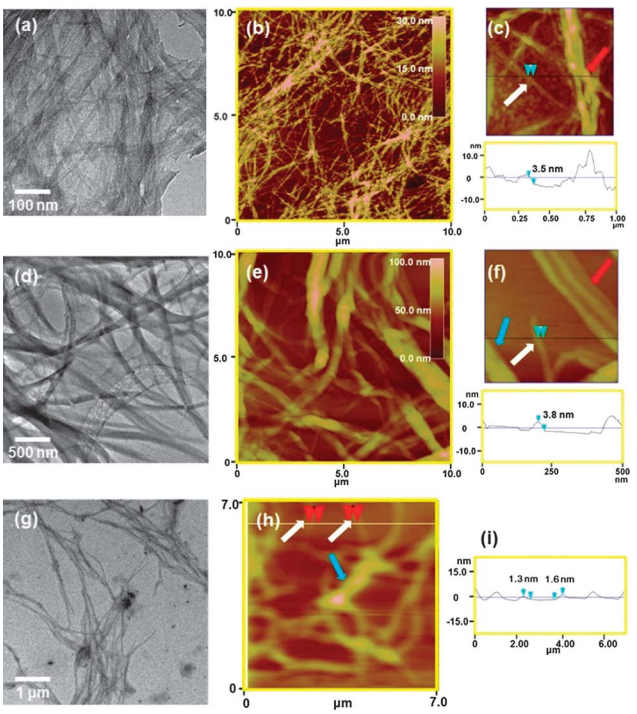

Fig. 7 TEM images, AFM height images, and AFM section analysis of (a, b and c) **1-TPP** and (d, e and f) **1-BTTPA** nanowires formed by diffusing CH_2Cl_2 to their THF solution (0.5 mg mL^{-1}). (g) TEM and (h and i) AFM height images and section analysis of **1-C12** nanowires drop-cast from dilute solution (for TEM, 10^{-5} M in THF; for AFM, 10^{-6} M in TCE).

Based all the results above, we conclude that: (1) the formation of the nanowires consists of two forces: along-wire hydrogen-bonding interactions and lateral van der Waals interactions; (2) the growth of the hydrogen-bonding nanowires needs a nucleation-elongation process, similar to other supramolecular polymerization processes; (3) the modification of the side groups affects the aggregation behaviours, which can be tuned by changing the solvent; (4) single molecular nanowires are obtained at high concentrations after introducing lateral bulky groups; (5) nanowires are formed by the packing of single molecular wires, and a fusion process may exist in the system. Accordingly, we illustrate the formation process of the nanowires as shown in Fig. 8 and propose that the formation mechanism contains four steps: (1) nucleation: a few molecules assembled together by hydrogen-bonding to form nuclei; (2) elongation: nuclei growth to form mesocale primary assemblies (known as nucleation-elongation polymerization); (3) oriented-attachment: primary assemblies packed together to form larger assemblies; (4) fusion: progressively adjusting their orientation and intermolecular packing to form final nanowires. Therefore, a prolonged solvent-annealing will provide a better crystallinity of the nanowires.

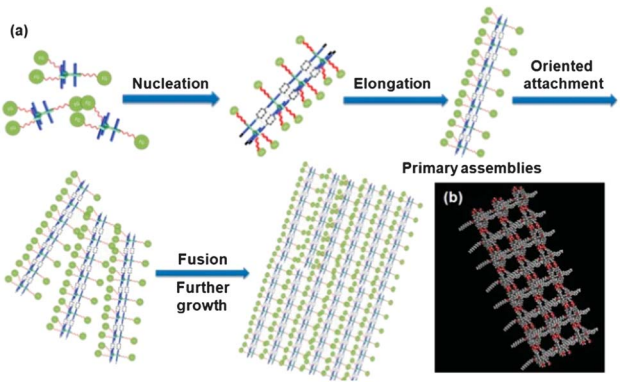

Fig. 8 (a) Proposed growth mechanism of the nanowires. (b) Molecular models of the aggregates of **1-C12**.

Conclusions

In summary, using XRD and HR-TEM, we carefully analyze the molecular packing mode of **1-C12** in the nanowires. We demonstrate that the nanowires are constructed with lots of single molecular wires *via* weak lateral interactions and arranged parallel to the substrate. This kind of molecular packing is analogous to a nematic phase, only having unidirectional periodicity. In order to understand the formation mechanism, we monitor the time-dependent size distributions *in situ* in the formation process of **1-C12** nanowires through DLS. The "S" curve suggests the occurrence of both nucleation and growth processes. The self-assembly process contains a kind of mesoscale assembly, which is thermodynamically stable both in dilute solution and at higher temperature. Such kind of size distributions suggests that the supramolecular polymerization and the nanowire growth are not isodesmic process. Based on these results, we first propose a three-step formation mechanism, in which such mesoscale assemblies are attributed to single molecular wires formed by hydrogen-bonding. After incorporating bulky groups at side chains, noticeable solvent effect on the self-assembly of the monomers is observed, and we think that the lateral growth tendency is mainly determined by the strength of the van der Waals interactions of the functional groups. *The weaker the interactions between the lateral groups and the stronger the interactions of the side groups with the solvent are, the more obvious the tendency to 1D growth.* The formation of single molecular wires in concentrated solutions is rarely reported in previous literature and is attributed to the weakened fusion process due to the rigid and bulky lateral groups. TEM and AFM images also give supportive proofs that the fusion process may be correlated within. Based on all above findings, we finally conclude that a four-step growth mechanism occurs, containing nucleation growth, elongation polymerization, oriented-attachment and a fusion process. Previous investigations proved that the supramolecular polymerization process had a nucleation-elongation process.[6–10] However, we focus on the latter part of nanowire growth—what happened after the supramolecular polymerization? This is the first time it has been demonstrated that after the supramolecular polymerization, oriented-attachment and fusion mechanism are both also critical process for the construction of large organic assemblies, such as ONWs.

Acknowledgements

This work was supported by the Major State Basic Research Development Program (No 2009CB623601) from the Ministry of Science and Technology, and National Natural Science Foundation of China.

Notes and references

1 (*a*) T. Lei and J. Pei, *J. Mater. Chem.*, 2012, **22**, 785; (*b*) F. S. Kim, G. Ren and S. A. Jenekhe, *Chem. Mater.*, 2011, **23**, 682; (*c*) P. Pramod, K. G. Thomas and M. V. George, *Chem.–Asian J.*, 2009, **4**, 806; (*d*) R. Li, W. Hu, Y. Liu and D. Zhu, *Acc. Chem. Res.*, 2010, **43**, 529; (*e*) Y. S. Zhao, H. Fu, A. Peng, Y. Ma, Q. Liao and J. Yao, *Acc. Chem. Res.*, 2010, **43**, 409; (*f*) L. Zang, Y. Che and J. S. Moore, *Acc. Chem. Res.*, 2008, **41**, 1596; (*g*) J. G. Rudick and V. Percec, *Acc. Chem. Res.*, 2008, **41**, 1641; (*h*) J. Wu, W. Pisula and K. Müllen, *Chem. Rev.*, 2007, **107**, 718; (*i*) A. P. H. J. Schenning and E. W. Meijer, *Chem. Commun.*, 2005, 3245.

2 (*a*) Y. Che, X. Yang, S. Loser and L. Zang, *Nano Lett.*, 2008, **8**, 2219; (*b*) Y. Che, A. X. Y. Datar, T. Naddo, J. Zhao and L. Zang, *J. Am. Chem. Soc.*, 2007, **129**, 6354.

3 (*a*) Q. Tang, Y. Tong, W. Hu, Q. Wan and T. Bjørnholm, *Adv. Mater.*, 2009, **21**, 4234; (*b*) T. Lei, Y. Zhou, C.-Y. Cheng, Y. Cao, Y. Peng, J. Bian and J. Pei, *Org. Lett.*, 2011, **13**, 2642; (*c*) Q. Tang, H. Li, Y. Liu and W. Hu, *J. Am. Chem. Soc.*, 2006, **128**, 14634.

4 (*a*) Y. Zhang, P. Chen, L. Jiang, W. Hu and M. Liu, *J. Am. Chem. Soc.*, 2009, **131**, 2756; (*b*) Y. Che, X. Yang, K. Balakrishnan, J. Zuo and L. Zang, *Chem. Mater.*, 2009, **21**, 2930; (*c*) Y. Zhou, L. Wang, J. Wang, J. Pei and Y. Cao, *Adv. Mater.*, 2008, **20**, 3745; (*d*) Y. S. Zhao, H. Fu, A. Peng, W. Yang and J. Yao, *Adv. Mater.*, 2008, **20**, 2859; (*e*) Y. Yamamoto, T. Fukushima, Y. Suna, N. Ishii, A. Saeki, S. Seki, S. Tagawa, M. Taniguchi, T. Kawai and T. Aida, *Science*, 2006, **314**, 1761.

5 T. Gulik-Krzywicki, C. Fouquei and J.-M. Lehn, *Proc. Natl. Acad. Sci. U. S. A.*, 1993, **90**, 163.

6 (*a*) D. Zhao and J. S. Moore, *J. Am. Chem. Soc.*, 2003, **125**, 16294; (*b*) D. Zhao and J. S. Moore, *J. Am. Chem. Soc.*, 2002, **124**, 9996.

7 D. Zhao and K. Yue, *Macromolecules*, 2008, **41**, 4029.

8 (*a*) P. Jonkheijm, P. van der Schoot, A. P. H. J. Schenning and E. W. Meijer, *Science*, 2006, **313**, 80; (*b*) V. Percec, G. Ungar and M. Peterca, *Science*, 2006, **313**, 55.

9 T. F. A. De Greef, M. M. J. Smulders, M. Wolffs, A. P. H. J. Schenning, R. P. Sijbesma and E. W. Meijer, *Chem. Rev.*, 2009, **109**, 5687.

10 (*a*) T. E. Kaiser, V. Stepanenko and F. Würthner, *J. Am. Chem. Soc.*, 2009, **131**, 6719; (*b*) F. Helmich, C. C. Lee, M. M. L. Nieuwenhuizen, J. C. Gielen, P. C. M. Christianen, A. Larsen, G. Fytas, P. E. L. Leclère, A. P. H. J. Schenning and E. W. Meijer, *Angew. Chem. Int. Ed.*, 2010, **43**, 3939.

11 Y. Zhou, W.-J. Liu, Y. Ma, H. Wang, L. Qi, Y. Cao, J. Wang and J. Pei, *J. Am. Chem. Soc.*, 2007, **129**, 12386.

12 J.-Y. Wang, J. Yan, L. Ding, Y. Ma and J. Pei, *Adv. Funct. Mater.*, 2009, **19**, 1746.

13 J. Yin, Y. Zhou, T. Lei and J. Pei, *Angew. Chem., Int. Ed.*, 2011, **50**, 6320.

14 J. A. Dirksen and T. A. Ring, *Chem. Eng. Sci.*, 1991, **46**, 2389.

15 W. F. Z. Ostwald, *Phys. Chem.*, 1897, **22**, 289.

16 (*a*) R. L. Penn and J. F. Banfield, *Science*, 1998, **281**, 969; (*b*) J. F. Banfield, S. A. Welch, H. Zhang, T. T. Ebert and R. L. Penn, *Science*, 2000, **289**, 751.

17 (*a*) Q. Zhang, S.-J. Liu and S.-H. Yu, *J. Mater. Chem.*, 2009, **19**, 191; (*b*) S.-F. Chen, J.-H. Zhu, J. Jiang, G.-B. Cai and S.-H. Yu, *Adv. Mater.*, 2010, **22**, 540.

18 (*a*) H. Cölfen and S. Mann, *Angew. Chem., Int. Ed.*, 2003, **42**, 2350; (*b*) M. Niederberger and H. Cölfen, *Phys. Chem. Chem. Phys.*, 2006, **8**, 3271.

19 (*a*) C. Burda, X. Chen, R. Narayanan and M. A. El-Sayed, *Chem. Rev.*, 2005, **105**, 1025; (*b*) S.-H. Yu, H. Cölfen, K. Tauer and M. Antonietti, *Nat. Mater.*, 2005, **4**, 51; (*c*) S.-H. Yu, M. Antonietti, H. Cölfen and J. Hartmann, *Nano Lett.*, 2003, **3**, 379.

20 (*a*) H. G. Yang and H. C. Zeng, *Angew. Chem., Int. Ed.*, 2004, **43**, 5930; (*b*) H. C. Zeng, *J. Mater. Chem.*, 2006, **16**, 649.

21 T. Tsuruoka, S. Furukawa, Y. Takashima, K. Yoshida, S. Isoda and S. Kitagawa, *Angew. Chem., Int. Ed.*, 2009, **48**, 4739.

22 (*a*) J. Luo, Y. Zhou, Z.-Q. Niu, Q.-F. Zhou, Y. Ma and J. Pei, *J. Am. Chem. Soc.*, 2007, **129**, 11314; (*b*) J. Luo, T. Lei, X. Xu, F.-M. Li, Y. Ma, K. Wu and J. Pei, *Chem.–Eur. J.*, 2008, **14**, 3860.

23 (*a*) J. Luo, T. Lei, L. Wang, Y. Ma, Y. Cao, J. Wang and J. Pei, *J. Am. Chem. Soc.*, 2009, **131**, 2076; (*b*) T. Lei, C.-Y. Cheng, Z.-H. Guo, C. Zheng, Y. Zhou, D. Liang and J. Pei, *J. Mater. Chem.*, 2012, **22**, 4306.

24 P. G. De Genes, J. Prost, *The Physics of Liquid Crystals (2nd Edition)*, Clarendon Press, Oxford, 1993.

25 (*a*) J. Zhang, D. Li, G. Liu, K. J. Glover and T. Liu, *J. Am. Chem. Soc.*, 2009, **131**, 15152; (*b*) G. Liu and T. B. Liu, *Langmuir*, 2005, **21**, 2713.

26 (*a*) J. K. G. Dhont, C. Smits and H. N. W. Lekkerkerker, *J. Colloid Interf. Sci.*, 1992, **152**, 386; (*b*) Y. Long, R. A. Shanks and Z. H. Stachurski, *Prog. Polym. Sci.*, 1995, **20**, 651; (*c*) W. Schärtl, *Light Scattering from Polymer Solutions and Nanoparticle Dispersions*, Springer, 2007.

27 Y. Miyamura, K. Kinbara, Y. Yamamoto, V. K. Praveen, K. Kato, M. Takata, A. Takano, Y. Matsushita, E. Lee, M. Lee and T. Aida, *J. Am. Chem. Soc.*, 2010, **132**, 3292.

28 M. Ma, Y. Kuang, Y. Gao, Y. Zhang, P. Gao and B. Xu, *J. Am. Chem. Soc.*, 2010, **132**, 2719.

